Prediction of Weak Topological Insulators in Layered Semiconductors

Binghai Yan,[1] Lukas Müchler,[1,2] and Claudia Felser[1,2]

[1]*Institute for Inorganic and Analytical Chemistry, Johannes Gutenberg University of Mainz, 55099 Mainz, Germany*
[2]*Max Planck Institute for Chemical Physics of Solids, D-01187 Dresden, Germany*

(Received 18 June 2012; published 13 September 2012)

We report the discovery of weak topological insulators by *ab initio* calculations in a honeycomb lattice. We propose a structure with an odd number of layers in the primitive unit cell as a prerequisite for forming weak topological insulators. Here, the single-layered KHgSb is the most suitable candidate for its large bulk energy gap of 0.24 eV. Its side surface hosts metallic surface states, forming two anisotropic Dirac cones. Although the stacking of even-layered structures leads to trivial insulators, the structures can host a quantum spin Hall layer with a large bulk gap, if an additional single layer exists as a stacking fault in the crystal. The reported honeycomb compounds can serve as prototypes to aid in the finding of new weak topological insulators in layered small-gap semiconductors.

DOI: 10.1103/PhysRevLett.109.116406 PACS numbers: 71.20.−b, 73.20.−r

Topological insulators (TIs) have attracted extensive research attention in the last few years [1–4]. They differ from normal insulators in that they exhibit gapless boundary states inside a bulk energy gap. In 2D, a TI has counterpropagating edge states with opposite spin that carry dissipationless current [5,6]. In 3D, TIs are further classified into strong and weak TIs according to the nature of their surface states [7–9]. A strong TI has metallic surface states that usually form an odd number of Dirac cones. The surface states are robust to perturbations that do not break the time-reversal (TR) symmetry. A weak TI is topologically equivalent to a stack of 2D TI layers; however, such a TI has an even number of Dirac cones on the side surface. Its surface states were initially assumed to be unstable with respect to disorders [7]; however, recent research [10,11] has revealed that surface states of a weak TI behave robustly even under strong TR-invariant disorders, similar to those of a strong TI.

The discovery of TI materials has stimulated intense research activity. The first experimentally observed TI was HgTe [5,6]. This compound exhibits an inverted band order between the conduction and valence bands (Hg-s and Te-p states), which determines its band topology. This intuitive band-inversion picture with the topological band theory [8,12–14] paved the way to the discovery of new TIs, including the Bi_2Se_3 [15–17], Heusler [18,19], and $TlBiSe_2$ [20–24] families. Nearly all reported TIs are either 2D TIs or 3D strong TIs; however, no weak TIs have been reported thus far. In this Letter, we report a method to design weak TIs using layered semiconductors. We employed the honeycomb lattice as an example. Several ternary compounds in the double-layered honeycomb lattice have previously been reported to be trivial insulators [25], although they exhibit band inversions. In our study, we used an odd number of layers in the primitive unit cell in order to realize an odd number of band inversions. Using this approach we discovered a family of weak TIs among ternary honeycomb compounds. Taking advantage of the tunability of the band structures of these compounds, we demonstrated a phase diagram including weak TIs, strong TIs, and trivial insulators.

The XYZ honeycomb compound can typically be viewed as honeycomb YZ layers with alternating hexagonal layers of X atoms stuffing between neighboring YZ layers. This is similar to the cubic XYZ Heusler compound (see Ref. [[26]] and references therein), in which Y and Z atoms form a zinc blende structure with the X atoms filling the void space of the lattice. The single-layered lattice has only one honeycomb layer in the primitive unit cell, and it exhibits no inversion symmetry. However, the double-layered lattice contains two honeycomb layers with a formula of $X_2Y_2Z_2$, in which two YZ layers are connected by the space inversion at X, as shown in Fig. 1. The low energy band structure is mainly related to the YZ honeycomb layer, while the X layer affects the coupling between the YZ layers. It is possible to create a YZ layer with an inverted band structure using heavy elements that have strong spin-orbit coupling (SOC). Such a layer leads to the formation of a 2D TI, also called a quantum spin Hall (QSH) insulator. By stacking such YZ layers along the z direction, we can obtain weak TIs [7] by retaining an odd number of layers in the primitive unit cell. Here, the odd-layered stacking induces an odd number of band inversions, which is necessary to realize topological nontrivial band structures.

In order to investigate band structures of the honeycomb compounds, we performed *ab initio* calculations within the framework of the density-functional theory (DFT). The exchange-correlation functional was within the generalized gradient approximation [27]. The core electrons were represented by the projector-augmented wave potential. We employed the Vienna *ab initio* simulation package with a plane wave basis [28]. First, we relaxed the lattice parameters and atomic positions for ternary compounds

XYZ ($X = K$, Na, Li; $Y = Hg$, Cd/Au, Ag; $Z =$ Sb, As, P/Te, Se). Here, XYZ follows the 18-valence electron rule (closed shell), in a manner similar to the Heusler compounds [18,26]. Subsequently, we calculated their band structures with SOC using these optimized structures. We should note that many ternary compounds in this family have already been synthesized in experiments. For example, KHgSb and KHgAs [29] are found to crystalize into the honeycomb lattice. Although LiAgSe and NaAgSe [30] have recently been reported to have lower energy in different structures by generalized gradient approximation calculations, we adopted the honeycomb phase of these two compounds for a full understanding of the topological phase transition with respect to element type.

We take KHgSb as an example of these compounds. As illustrated in Fig. 1(d), the Hg-s and Sb-p states are located near E_F, in which Hg-s is lower than Sb-p. Under the crystal field, Sb-p splits into the p_{xy} and p_z states with p_{xy} being degenerate at E_F. When applying SOC, the p_{xy} states split again into $j = 3/2$ and $j = 1/2$ states, thereby causing the formation of a finite energy gap. Then we can see a band inversion between Hg-s ($j = 1/2$) and Sb-p_{xy} ($j = 3/2$) states, which occurs only at the Γ point of the 2D Brillouin zone. This inversion is confirmed by our DFT calculations. This results in a nontrivial topological $\mathbb{Z}_2$ index of $\nu = 1$, according to the $\mathbb{Z}_2$ classification [7,9]. Therefore, an isolated KHgSb layer is a 2D TI with an inverted band structure, similar to HgTe quantum wells. Next, we stack the isolated KHgSb layer along the z direction (perpendicular to the surface) into a 3D lattice. If a primitive unit cell contains only one KHgSb unit, we refer to it as an A-A stacking, where A denotes a single KHgSb layer. If the unit cell contains two KHgSb units, we refer to it as an AA'-AA' stacking, where A' represents an inverted A layer with the K atom as the inversion center. An A-A stacking of KHgSb is the simplest case. Here, the interlayer coupling is weak. Consequently, the band dispersion along the Γ-Z (also called A) direction is extremely small. Hence, the band inversion remains at both the Γ and Z points. As shown in Fig. 2(a), the Hg-s and Sb-p_{xy} band inversion happens twice with one inversion occurring at the Γ point and the other occurring at the Z point. In Fig. 1(c), eight time reversal invariant momenta (TRIM) Γ_i ($i = 1, 2, \ldots, 8$) are labeled as Γ, Z, $M_{1,2,3}$, and $L_{1,2,3}$. According to Fu and Kane's method [7,9], the quantity δ_i is -1 if an odd number of band inversions occur at Γ_i; otherwise, δ_i is $+1$. (When the crystal structure has inversion symmetry, δ_i is the product of parity eigenvalues of the valence bands at Γ_i.) Consequently, the single-layered KHgSb has $\sigma_\Gamma = \sigma_Z = -1$ and $\sigma_{M_{1,2,3}} = \sigma_{L_{1,2,3}} = +1$. The main topological index ν_0 of $\mathbb{Z}_2$ ($\nu_0;\nu_1\nu_2\nu_3$) is determined by $(-1)^{\nu_0} = \prod_i \sigma_i$. The other three indices are determined as $(-1)^{\nu_1} = \sigma_{M_1}\sigma_{M_2}\sigma_{L_1}\sigma_{L_2}$, $(-1)^{\nu_2} = \sigma_{M_2}\sigma_{M_3}\sigma_{L_2}\sigma_{L_3}$, and $(-1)^{\nu_3} = \sigma_{L_1}\sigma_{L_2}\sigma_{L_3}\sigma_Z$. In other words, ν_0 corresponds to all eight TRIM; $\nu_{1,2,3}$ correspond to four TRIM on a surface that does not include the Γ point, where the surface belongs to the parallelepiped [see Fig. 1(c)] formed by these eight TRIM. Thus, the single-layered KHgSb belongs to the $\mathbb{Z}_2$ (0;001) class of weak TIs. Here, [001] also indicates the stacking direction of the QSH layers. The energy gap at Γ, which is approximately 0.5 eV, is determined by the SOC splitting of the Sb-p states. The s-p band inversion strength at Γ, which is approximately 1.5 eV, is related to the energy level difference between the Hg-s and Sb-p states. In addition, we also performed GW calculations [31] with self-energy corrections to the DFT band structures. The band inversion is preserved in the GW band structure, which confirms the topological feature of this material.

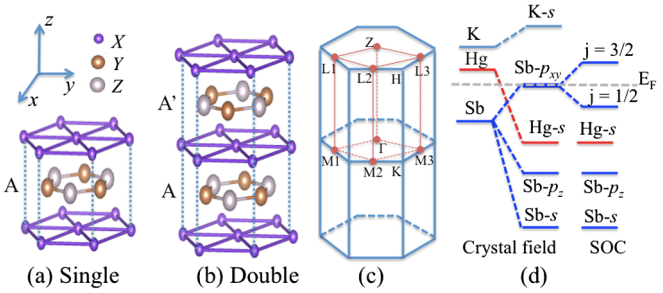

FIG. 1 (color online). Crystal structures of honeycomb compound XYZ. The single-layered structure (a) contains only one XYZ layer, while the double-layered one (b) includes two XYZ layers. These two XYZ layers in (b) are labeled as A and A', which are related to each other by an inversion with one X atom as the inversion center. (c) The Brillouin zone of the honeycomb lattice. Eight time reversal-invariant-momenta are denoted by orange dots that form a parallelepiped. (d) The band evolution at the Γ point of the single-layered KHgSb. Under crystal field without SOC, Sb-p_{xy} states are degenerate at the Fermi energy and the Hg-s state is below these degenerate states. After applying SOC, Sb-p_{xy} splits into $j = 3/2$ and $j = 1/2$ states, thereby resulting in a gapped insulator with inverted bands between Hg-s and Sb-p_{xy} ($j = 3/2$).

As seen above, the 2D KHgSb layer has an s-p band inversion similar to that of HgTe. Bernevig, Hughes, and Zhang (BHZ) [5] have previously written a $k \cdot p$ Hamiltonian for HgTe quantum wells. Hence, we can

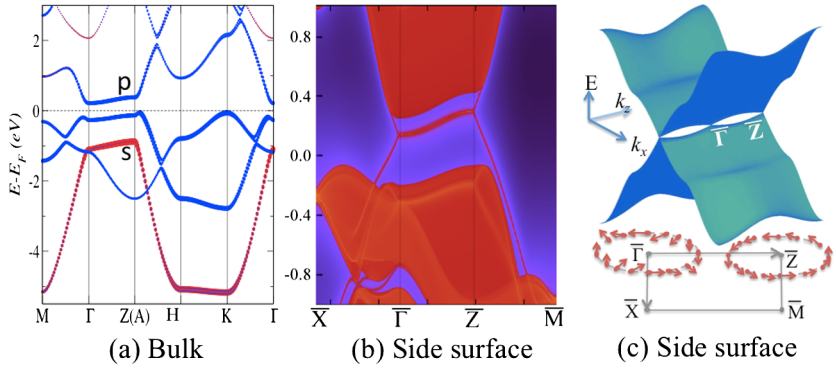

(a) Bulk (b) Side surface (c) Side surface

FIG. 2 (color online). (a) Bulk band structures of single-layered KHgSb. The Hg-s state is highlighted by filled red circles and Sb-p states by filled blue circles. The size of circles indicates the amount of the corresponding s or p character. The surface states on the side surface (xz) of KHgSb were calculated (b) by the tight-binding Wannier function method and (c) by the $k \cdot p$ method. Two Dirac cones exist at the $\bar{\Gamma}$ and $\bar{Z}$ points, respectively. The spin texture is also plotted for these two Dirac cones in (c), where the Fermi surface is above two Dirac points.

describe this QSH layer by the BHZ model. When stacking the QSH layers into 3D, we added the k_z term to the BHZ model and obtained the Hamiltonian for our weak TIs, expressed on the basis of $\{|s; j = 1/2, m_j = 1/2>, |p; j = 3/2, m_j = 3/2>, |s; j = 1/2, m_j = -1/2>, |p; j = 3/2, m_j = -3/2>\}$,

$$H(k) = \epsilon(k)\mathbb{I}_{4\times 4} + \begin{pmatrix} M(k) & Ak_+ & 0 & Ek_z \\ Ak_- & -M(k) & Fk_z & 0 \\ 0 & Fk_z & M(k) & -Ak_- \\ Ek_z & 0 & -Ak_+ & -M(k) \end{pmatrix}, \quad (1)$$

where $E(k) = C + Dk^2$ and $M(k) = M - B(k_x^2 + k_y^2) - Gk_z^2$. We used a minimal four-band model, and the split-orbit split-off bands ($j = 1/2$) are neglected, for they are not involved into the band inversion. Here, M in $M(k)$ denotes the intralayer band inversion strength, and Gk_z^2, Ek_z, and Fk_z are related to the interlayer interaction. This $k \cdot p$ model holds for both the Γ and Z points due to weak k_z dispersion. As a simple example, Eq. (1) represents a QSH layer when $C = D = 0$, $A = 1$, $B = -1$, $M = -2$, and $G = E = F = 0$. The compound becomes a weak TI when we initiate the interlayer coupling by setting $G = -0.1$, $E = F = 0.1$. We subsequently transferred the above continuum model to a tight-binding lattice and solved the surface band structure on a slab configuration. The anisotropic surface states are displayed on the entire 2D Brillouin zone, showing two Dirac points similar to those obtained from our *ab initio* calculations [see Figs. 2(b) and 2(c)]. We showed the spin texture of these two Dirac cones in Fig. 2(c). The Fermi surface above the Dirac points exhibits a vortex for each Dirac cone. Spin rotates oppositely between these two vortices; i.e., the vortex at $\bar{\Gamma}$ has index -1 and the other at $\bar{Z}$ has index $+1$. Therefore, the total Berry phase is zero when an electron travels a circle around the whole Brillouin zone.

The above model provides a tool to investigate the phase diagram of the interplay between the band inversion strength (characterized by M) and the interlayer coupling (mainly characterized by G), as illustrated in Fig. 3(a). One can also find strong TIs in honeycomb-lattice compounds, other than weak TIs and trivial insulators. The band structure of NaCdSb is shown in Fig. 3(c) as an example. Band inversion appears at the Γ point, while it disappears at Z because of considerable k_z dispersion of the s band. However, the system becomes a topological semimetal, instead of forming a real insulator. Here, the presence of threefold rotational symmetry induces band crossing between Γ and Z, and an energy gap can form when this symmetry is broken (e.g., by in-plane strain) [25]. We listed all the materials of the single-layered lattice in the phase diagram according to our *ab initio* calculations. As shown in Fig. 3(b), the heaviest compounds are usually weak TIs ($M < 0$, $G < 0$), the lightest ones are trivial insulators ($M > 0$), and in between them are strong TIs ($M < 0$, $G << 0$). In $XAgZ$ compounds, strong TIs exist among the lightest compounds. This is because the Ag-d states hybridize with Ag-s and $Z - p$ states and violate the simple $s - p$ picture slightly. As mentioned previously, all strong TIs are semimetals. Most weak TIs are also found to be semimetallic, though they usually have a finite direct energy gap throughout the Brillouin zone. Among weak TIs, KHgSb and KHgAs have full energy gaps of 0.24 and 0.05 eV, respectively.

The single-layered honeycomb lattice of KHgSb exhibits $s - p$ band inversions once at Γ and once at Z, as discussed above. This picture can be generalized to multilayered structures within the weak coupling limit. As indicated by the calculated band structures in Fig. 4(a), the double-layered structure with $AA' - AA'$ stacking has band inversions twice at Γ and twice at Z. Here, two Sb-p bands exist at the conduction band bottom, while two Hg-s bands appear in the valence bands. Thus, the double-layered KHgSb is a trivial insulator with $\mathbb{Z}_2$ (0;000), consistent

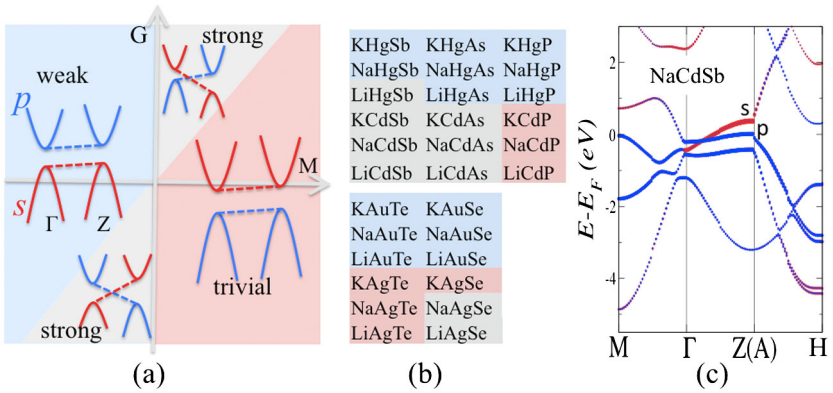

FIG. 3 (color online). (a) Phase diagram with respect to band inversion strength M and interlayer coupling G. The band inversions at Γ and Z are illustrated for the single-layered lattice. The dashed lines denote the band dispersion along the $\Gamma - Z$ direction. The red (blue) solid lines indicate the s (p) band dispersion in the k_x k_y plane around the Γ and Z points. (b) All single-layered XYZ compounds in this family are classified into weak TIs (light blue), strong TIs (gray), and trivial insulators (pink). (c) The band structure of the single-layered bulk NaCdSb is shown as an example of a strong TI. The band inversion between the s (red dots) and p (blue dots) states occurs at Γ, but disappears at Z.

with our previous results obtained from the parity criteria [25]. Furthermore, the triple-layered structure with $AA'A-AA'A$ stacking is a weak TI again, due to inversion occurring thrice [see Fig. 4(b)] at Γ and Z, respectively. Therefore, we can expect an oscillation transition from a trivial insulator to a weak TI when the primitive unit cell changes from an even- to an odd-layered stacking. This even-odd transition is also consistent with the results of a recent phenomenological study by Ringel *et al.* [10] and Mong *et al.* [11]. If we treat the double (even)-layered structure as a period-doubling reconstruction [10,11] of a single (odd)-layered lattice, the scattering between two original Dirac cones will localize the surface states and induce a gapped trivial surface. On the other hand, in realistic materials the existence of disorder in the honeycomb plane can possibly eliminate the difference between A and A' layers, thereby giving rise to an equivalent A-A stacking lattice. Therefore, strong disorders in layered structures may probably induce weak TIs, rather than destroy them.

In the weak TI, a 1D helical state has previously been proposed to exist along the dislocation line of the lattice, which is protected by TR symmetry and is stable against weak disorder [33,34]. Our layered honeycomb compounds can provide an ideal platform to realize this proposal when dislocation defects exist. Another interesting topological defect is the stacking fault in the layered structure [illustrated in Fig. 4(c)]. For example, in a double-layered trivial insulator a stacking fault occurs in the sequence $AA' - AA' - A - AA' - AA'$. Consequently, the A layer is sandwiched between gapped trivial insulators, and it emerges as a nontrivial QSH layer. This is also consistent with the results of recent work by Liu *et al.* [35]. If we consider the $AA' - AA'$ sequence as a charge density wave perturbation on the A-A stacked lattice, the stacking fault is equivalent to the domain wall of two charge density waves. This type of domain wall was proposed to accommodate a QSH state [35]. In this sense, topological stacking faults in a trivial honeycomb material may offer a platform to realize the QSH effect. In KHgSb, the QSH layer has a large bulk energy gap of approximately 0.2 eV. Therefore, topological edge states can be measured even at room temperature.

In conclusion, we predicted the first weak topological insulators by designing odd-layered structures in the honeycomb lattice using *ab initio* band structure calculations. The most suitable candidate in this family is the single-layered KHgSb, which is a weak TI with a large bulk energy gap of 0.24 eV. Even the trivial insulators in this family, i.e., even-layered compounds, can host a quantum spin Hall layer, when a stacking fault occurs in the crystal.

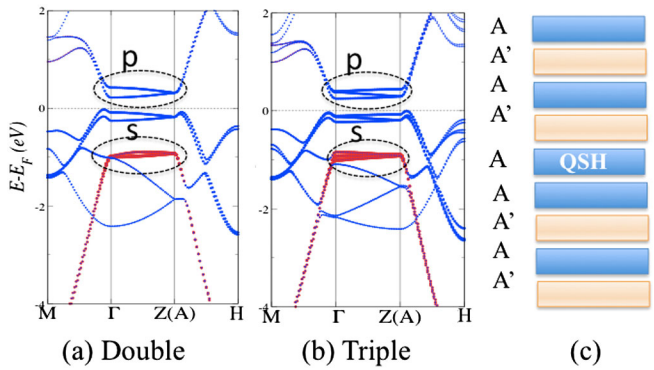

FIG. 4 (color online). Bulk band structures of (a) double-layered KHgSb and (b) triple-layered KHgSb. Filled red circles denote Hg-s states while blue circles indicate Sb-p states. The inverted Hg-s and Sb-p bands are highlighted by dashed circles. Band inversions occur twice and thrice in (a) and (b), respectively. (c) The stacking fault in the honeycomb lattice. In a trivial insulator with $AA' - AA'$ stacking, an extra A layer as a stacking fault can become a quantum spin Hall layer.

The reported honeycomb lattice can be a prototype to find new weak TIs in layered semiconductors, in which the method of odd-layered structures can be applied.

We are indebted to Dr. H. J. Zhang and Professor S.-C. Zhang at Stanford University, Professor J. Kübler at Technische Universität Darmstadt, Professor J. Mydosh at Universität zu Köln, and Professor C. X. Liu at Pennsylvania State University for their great help. B. Y. gratefully acknowledges funding by the DFG project SPP 1458.

[1] X.-L. Qi and S.-C. Zhang, Phys. Today **63**, No. 1, 33 (2010).
[2] J. Moore, Nature (London)**464**, 194 (2010).
[3] M. Z. Hasan and C. L. Kane, Rev. Mod. Phys. **82**, 3045 (2010).
[4] X.-L. Qi and S.-C. Zhang, Rev. Mod. Phys. **83**, 1057 (2011).
[5] B. A. Bernevig, T. L. Hughes, and S. C. Zhang, Science **314**, 1757 (2006).
[6] M. König, S. Wiedmann, C. Brüne, A. Roth, H. Buhmann, L. Molenkamp, X.-L. Qi, and S.-C. Zhang, Science **318**, 766 (2007).
[7] L. Fu and C. L. Kane, Phys. Rev. B **76**, 045302 (2007).
[8] J. E. Moore and L. Balents, Phys. Rev. B **75**, 121306 (2007).
[9] L. Fu, C. L. Kane, and E. J. Mele, Phys. Rev. Lett. **98**, 106803 (2007).
[10] Z. Ringel, Y. Kraus, and A. Stern, Phys. Rev. B **86**, 045102 (2012).
[11] R. S. K. Mong, J. H. Bardarson, and J. E. Moore, Phys. Rev. Lett. **108**, 076804 (2012).
[12] C. L. Kane and E. J. Mele, Phys. Rev. Lett. **95**, 226801 (2005).
[13] L. Fu and C. L. Kane, Phys. Rev. B **74**, 195312 (2006).
[14] R. Roy, Phys. Rev. B **79**, 195321 (2009).
[15] H.-J. Zhang, C.-X. Liu, X.-L. Qi, X. Dai, Z. Fang, and S.-C. Zhang, Nature Phys. **5**, 438 (2009).
[16] Y. Xia, D. Qian, D. Hsieh, L. Wray, A. Pal, H. Lin, A. Bansil, D. Grauer, Y. S. Hor, R. J. Cava, and M. Z. Hasan, Nature Phys. **5**, 398 (2009).
[17] Y. L. Chen, J. G. Analytis, J.-H. Chu, Z. K. Liu, S.-K. Mo, X. L. Qi, H. J. Zhang, D. H. Lu, X. Dai, Z. Fang, S. C. Zhang, I. R. Fisher, Z. Hussain, and Z.-X. Shen, Science **325**, 178 (2009).
[18] S. Chadov, X.-L. Qi, J. Kübler, G. H. Fecher, C. Felser, and S.-C. Zhang, Nature Mater. **9**, 541 (2010).
[19] H. Lin, L. A. Wray, Y. Xia, S. Xu, S. Jia, R. J. Cava, A. Bansil, and M. Z. Hasan, Nature Mater. **9**, 546 (2010).
[20] B. Yan, C.-X. Liu, H.-J. Zhang, C.-Y. Yam, X.-L. Qi, T. Frauenheim, and S.-C. Zhang, Europhys. Lett. **90**, 37002 (2010).
[21] T. Sato, K. Segawa, H. Guo, K. Sugawara, S. Souma, T. Takahashi, and Y. Ando, Phys. Rev. Lett. **105**, 136802 (2010).
[22] K. Kuroda, M. Ye, A. Kimura, S. V. Eremeev, E. E. Krasovskii, E. V. Chulkov, Y. Ueda, K. Miyamoto, T. Okuda, K. Shimada, H. Namatame, and M. Taniguchi, Phys. Rev. Lett. **105**, 146801 (2010).
[23] Y. L. Chen, Z. K. Liu, J. G. Analytis, J.-H. Chu, H. J. Zhang, B. H. Yan, S.-K. Mo, R. G. Moore, D. H. Lu, I. R. Fisher, S. C. Zhang, Z. Hussain, and Z.-X. Shen, Phys. Rev. Lett. **105**, 266401 (2010).
[24] H. Lin, R. S. Markiewicz, L. A. Wray, L. Fu, M. Z. Hasan, and A. Bansil, Phys. Rev. Lett. **105**, 036404 (2010).
[25] H.-J. Zhang, S. Chadov, L. Müchler, B. Yan, X.-L. Qi, J. Kübler, S.-C. Zhang, and C. Felser, Phys. Rev. Lett. **106**, 156402 (2011).
[26] T. Graf, C. Felser, and S. Parkin, Prog. Solid State Chem. **39**, 1 (2011).
[27] J. P. Perdew, K. Burke, and M. Ernzerhof, Phys. Rev. Lett. **77**, 3865 (1996).
[28] G. Kresse and J. Hafner, Phys. Rev. B **47**, 558 (1993).
[29] R. Vogel and H.-U. Schuster, Z. Naturforsch. **35B**, 114 (1980).
[30] J. Vidal, X. Zhang, L. Yu, J. W. Luo, and A. Zunger, Phys. Rev. B **84**, 041109(R) (2011).
[31] M. Shishkin and G. Kresse, Phys. Rev. B **74**, 035101 (2006).
[32] N. Marzari and D. Vanderbilt, Phys. Rev. B **56**, 12847 (1997).
[33] Y. Ran, Y. Zhang, and A. Vishwanath, Nature Phys. **5**, 298 (2009).
[34] K. I. Imura, Y. Takane, and A. Tanaka, Phys. Rev. B **84**, 035443 (2011).
[35] C.-X. Liu, X.-L. Qi, and S.-C. Zhang, Physica (Amsterdam) **44E**, 906 (2012).